Mechanics of Advanced Composite Structures 8 (2021) 389 – 399

Mechanics of Advanced Composite Structures

Semnan University

journal homepage: http://MACS.journals.semnan.ac.ir

Application of Bi-Directional Functionally Graded Material Model for Free Vibration Analysis of Rotating Euler-Bernoulli Nanobeams

S. M. K. Ohab-Yazdi and M. Kadkhodayan*

Department of Mechanical Engineering, Ferdowsi University of Mashhad, Mashhad, Iran

KEYWORDS

Rotating nanobeam
Generalized differential quadrature method
Nonlocal elasticity theory

ABSTRACT

In this work, mechanical vibration analysis of rotating bi-directional functionally graded Euler-Bernoulli nanobeams is investigated, which has not already been studied deeply based on the latest authors' knowledge. Material properties vary along the thickness and axis directions based on power-law distribution. The nonlocal elasticity theory of Eringen (NET) is utilized for modeling small-scale effects. Different boundary conditions are considered as clamped-clamped (C-C), clamped-simply (C-S), and clamped-free (C-F). Governing equations and associated boundary conditions are derived based on minimum total potential energy, and the generalized differential quadrature (GDQ) method is employed for the solution process. Convergence and verification studies are accomplished to affirm this work, and in the continuation, the effects of various parameters, namely hub ratio, rotation speed, and power indexes along x and z directions on the dimensionless natural frequencies, are investigated. It is revealed that the decrement made by the different values of n_x in the natural frequency, parameter is more effective than the reduction caused by the n_z, especially for the higher rotation speed.

1. Introduction

Beams and columns made of functionally graded materials have been found in many different crafts such as civil, mechanical, and aerospace engineering and so on for the reason of desirable performance, namely eliminating delamination unfavorable events due to loading conditions, high strength to weight ratio, high corrosion and heat resistance, high machining capability. It is expected to expire the bending [1, 2] vibration [3-7] and buckling [8] analyses of beams and columns due to their simplicity and vast application for many years in the endurance of compressive and tensile forces and also as more than three decades go by introducing the concept of functionally graded materials [9]. However, their studies are the best topics of researchers even until now, and research is tracked to fill the gaps. Sherafatnia et al. [10] extended an analytical solution for the free vibration and buckling analysis of functionally graded material beams with edge cracks. They used different theories such as Euler-Bernoulli, Rayleigh, shear, and Timoshenko. Due to the hard operating situations, namely temperature and stress distribution in two or three directions, it is necessary to analyze the structures made of multi-directional functionally graded materials. Moreover, in practical cases, material properties vary in multi-direction [11-13]. Li Li et al.[14] developed the nonlinear bending behavior of bi-directional functionally graded Euler-Bernoulli beam throughout the GDQ method. They [15] also extended the free torsional vibration behavior of nanotubes made of a bi-directional functionally graded material model. Properties were supposed to change along the length and radius directions based on exponential and power-law distribution functions, respectively. It is found that the torsional frequencies are increased by decreasing the nonlocal parameter.

The rotation effect on the natural frequency is the most important parameter with various

*Corresponding author. Tel.: +98 9153111869 ; Fax: +98 5118763304
E-mail address: Kadkhoda@um.ac.ir

DOI: 10.22075/MACS.2021.21231.1300
Received 20-09-01; Received in revised form 21-08-08; Accepted 21-11-18

applications in engineering science, such as gas turbines, helicopter rotors, and wind turbines. Rotary structures have more complicated behavior than static ones, which is because of the rotation parameter. Therefore, vast efforts have been made to analyze these structures in recent years [16-19]. The static and dynamic analyses of micro-nano structures have attracted the consideration of engineering scientists with the increase of the usage of nano-electromechanical systems in the automotive industry. However, it is not accurate to apply classical theories for the analysis of micro-nano structures. On the other hand, dynamic simulations implementation on the nanostructures is computationally expensive. Thus the usage of size-dependent theories is suggested. Up to now, various size-dependent theories such as the modified couple stress theory (MCST) [20, 21], the modified strain gradient theory (MSGT) [22, 23], the NET [24, 25] and the nonlocal strain gradient theory (NSGT) [26-28] are proposed.

In 2016, Ebrahimi and Shafiei [29] performed the free vibration of rotating functionally graded nano cantilever beam with the aid of the GDQ method. After that, researchers have performed much research on the vibration of micro-nano rotating beams made of functionally graded materials based on MCST, MSGT, and NET. Karamanli and Aydogdu [30] exploited a bi-directional functionally graded porous sandwich materials model on the rotating microbeams. In their research, a four-variable refined and normal deformation beam theory was used based on MCST via the finite element method.

The GDQM is a precise and accurate method that can simple formulation while solving equations with low computational operations. In general, this method's simplicity and high accuracy are the most prominent characteristics of the GDQ method. Many researchers have been performed their studies with the aid of the GDQ method [31-34].

By considering the surveyed literature review, it can be concluded that there is no comprehensive research on the simultaneous effect investigation of axial functionally graded (AFG) and conventional functionally graded (CFG) power indexes and angular velocity on the free vibration of Euler-Bernoulli nanobeam via NET. The first accomplished works on the free [35] and forced [36] vibrations of isotropic rotary nanobeams and free vibration of rotary FG [29] nanobeam has been performed with cantilever boundary conditions. Therefore, to fill the detected gap, the free vibration of two-dimensional functionally graded material rotary nanobeam is presented here under C-C, C-S, and C-F boundary conditions employing the GDQ method. Material properties vary in both axial and thickness directions according to the power-law distribution. Numerical results indicate that increasing the AFG and CFG indexes decreases the first natural frequency. In C-C and C-S boundary conditions, it is observed that the stiffness-softening effect switches to the stiffness-hardening effect. But increasing the rotary speed in the C-F boundary condition vanishes the effect of the AFG index on the natural frequency. Moreover, with increasing the angular velocity, the effect of the functionally gradient index along x-direction on the natural frequency is more noticeable than that of the z-direction.

2. Theory and Formulation

A rotating Euler-Bernoulli nanobeam made of bi-directional functionally graded is considered as shown in Fig. 1. The Cartesian coordinate system is set at the end of the beam connected to a rigid hub such that its x-axis is taken perpendicular to the cross-sectional area of the beam. L, Ω, and R are total length, constant angular velocity, and hub radius.

2.1. Bi-directional functionally graded material model

The material properties are varied in both axial and thickness directions according to the power-law distribution [32, 33, 37] as follows:

$$\begin{cases} E(x,z) = E_m + (E_c - E_m) \times \left(\frac{1}{2} + \frac{z}{h}\right)^{n_z} \times \left(\frac{x}{L}\right)^{n_x} \\ \rho(x,z) = \rho_m + (\rho_c - \rho_m) \times \left(\frac{1}{2} + \frac{z}{h}\right)^{n_z} \times \left(\frac{x}{L}\right)^{n_x} \end{cases} \quad (1)$$

where E_m, E_c, ρ_m and ρ_c are Young's modulus and density of metal and ceramic, respectively and n_x and n_z denote the AFG and CFG indexes. It is also mentioned that Poisson's ratio is assumed to be constant. If n_x is set to zero, the nanobeam is made of conventional FGMs, and if n_x and n_z are set to zero simultaneously, the nanobeam is made of pure ceramic.

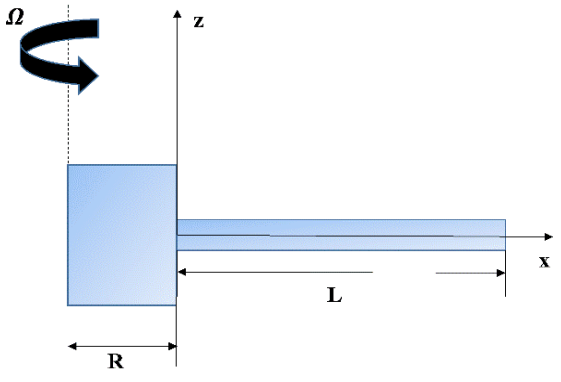

Fig. 1. The geometry of rotary Euler-Bernoulli nanobeam

2.2. Formulation of BD-FG rotary Euler-Bernoulli nanbeam model

According to Euler-Bernoulli nanobeam, $u_x(x,z,t)$ and $u_z(x,z,t)$ are the displacement fields of an arbitrary point of the beam along *x* and *z* directions which are described by:

$$\begin{cases} u_x(x,z,t) = u(x,t) - z\dfrac{\partial w}{\partial x} \\ u_z(x,z,t) = w(x,t) \end{cases} \tag{2}$$

in which *u(x,t)* and *w(x,t)* show the displacements of the central plane along with *x* and *z* directions, respectively. Based on the Euler-Bernoulli displacement field with two unknown, the linear strain-displacement relation are obtained by the following equation:

$$\varepsilon_{xx} = \frac{\partial u}{\partial x} - z\frac{\partial^2 w}{\partial x^2} \tag{3}$$

Hamilton's principle is used to derive the equations and related boundary conditions as follows:

$$\int_0^t \delta(U - T + V)dt = 0 \tag{4}$$

where *U, T,* and *V* are strain, kinetic and potential energies due to constant angular speed around the *z*-axis. The variation of strain energy is:

$$\delta U = \int \sigma_{ij}\delta\varepsilon_{ij}dV = \int_0^L \left(N\frac{\partial \delta u}{\partial x} - M\frac{\partial^2 \delta w}{\partial x^2}\right)dx \tag{5}$$

where N and M are the axial compressive force and bending moment, respectively as follows:

$$(N(x), M(x)) = \iint (1, z)\sigma_{xx}dA(x) \tag{6}$$

According to linear elastic solids, the constitutive equation for FG material can be expressed as:

$$\sigma_{xx}(x,z) = E(x,z)\varepsilon_{xx} \tag{7}$$

and the variation of kinetic energy is

$$\begin{aligned} &\delta T = \int \rho(x,z)u_{i,t}\delta u_{i,t}dV \\ &= \int_0^L \left(I_0(x)\left(\frac{\partial u}{\partial t}\frac{\partial \delta u}{\partial \delta t} + \frac{\partial w}{\partial t}\frac{\partial \delta w}{\partial \delta t}\right)\right. \\ &-I_1(x)\left(\frac{\partial \delta u}{\partial t}\frac{\partial^2 w}{\partial t \partial x} + \frac{\partial u}{\partial t}\frac{\partial^2 \delta w}{\partial t \partial x}\right) \\ &\left.+I_2(x)\left(\frac{\partial^2 \delta w}{\partial t \partial x}\frac{\partial^2 w}{\partial t \partial x}\right)\right)dx \end{aligned} \tag{8}$$

where $I_0(x), I_1(x), I_2(x)$ are the mass moments of inertia, defined as:

$$(I_0(x), I_1(x), I_2(x)) = \int (1, z, z^2)\rho(x,z)dA(x) \tag{9}$$

The variation of potential energy corresponding to the angular velocity can be written as:

$$\delta V = \int_0^L (N^R)\frac{\partial w}{\partial x}\frac{\partial \delta w}{\partial x}dx \tag{10}$$

where N^R is the rotational force and the following equation determines it:

$$N^R(x) = \int_x^L \iint_A \rho(\zeta, z)dA(\zeta) \times \Omega^2(R + \zeta)d\zeta \tag{11}$$

By inserting relations 8, 9, and 11 into hamilton's principle, performing some mathematical manipulation, and setting the coefficients of δu and δw to zero, the governing equations and related boundary conditions can be obtained by following equations:

$$\begin{aligned} &\delta u: \quad \frac{\partial N(x)}{\partial x} = I_0(x) \times \ddot{u} - I_1(x) \times \frac{\partial \ddot{w}}{\partial x} \\ &\delta w: \quad \frac{\partial^2 M(x)}{\partial x^2} + \frac{\partial}{\partial x}\left(N^R(x) \times \frac{\partial w}{\partial x}\right) \\ &= I_0(x) \times \ddot{w} + \frac{\partial}{\partial x}(I_1(x) \times \ddot{u}) - \frac{\partial}{\partial x}(I_2(x) \times \frac{\partial \ddot{w}}{\partial x}) \end{aligned} \tag{12}$$

with the related boundary conditions (at *x*=0, *L*)

2.3. Eringen nonlocal elasticity theory for FG nanobeam

$$\begin{aligned} &N(x) = 0 \ \ or \ \ \delta u = 0 \ \ at \ \ x = 0, L \\ &\frac{\partial M(x)}{\partial x} + N^R(x) \times \frac{\partial w}{\partial x} - I_1(x) \times \ddot{u} + I_2(x) \times \frac{\partial \ddot{w}}{\partial x} \\ &= 0 \ \ or \ \ \delta w = 0 \ \ at \ \ x = 0, L \\ &M(x) = 0 \ \ or \ \ \frac{\partial w}{\partial x} = 0 \ \ at \ \ x = 0, L \end{aligned} \tag{13}$$

NET is an appropriate theory for the analysis of nanostructures propounded by Eringen [38]. In this theory, the empty spaces between atoms are considered by small-scale parameters. Based on this theory, the stress of each arbitrary point *x* is supposed to be a function of the strain of all the points in the vicinity of *x*. Hence, the nonlocal stress tensor at any point *x* is defined as:

$$\sigma_{ij}^{nl}(x) = \int_\Gamma \alpha(|x' - x|, \tau)\, t_{ij}d\Gamma(x') \tag{14}$$

where, t_{ij} is local stress tensor. $\alpha(|x' - x|)$ denotes nonlocal kernel function and $\tau = \frac{e_0 a}{l}$ shows a material constant for applying the small scale factor, where e_0 is a material constant obtained experimentally, a and l represent internal and external characteristic lengths of the nanobeam, respectively. The local stress t_{ij} is defined based on Hook's law as:

$$t_{ij} = C_{ijkl}\varepsilon_{kl} \tag{15}$$

According to the differential form of nonlocal elasticity theory proposed by Eringen and due to the complexity of integral form, the only stress relation based on Euler-Bernoulli nonlocal functionally graded material is obtained as :

$$\sigma_{xx}^{nl}(x,z) - (e_0 a)^2\frac{\partial^2 \sigma_{xx}^{nl}(x,z)}{\partial x^2} = E(x,z)\varepsilon_{xx} \tag{16}$$

Multiplying $\iint_A dA$ and $\iint_A ZdA$ on relation. (16) yield to stress resultants. The governing equations of the nanobeam made of bidirectional functionally graded materials in terms of the

displacements are obtained by substituting the stress resultants in equations 12 and 13, as follows:

$$\begin{aligned}
&\delta u: \quad \frac{\partial}{\partial x}\left(A_{xx}(x)\frac{\partial u}{\partial x}\right)-\frac{\partial}{\partial x}\left(B_{xx}(x)\frac{\partial^2 w}{\partial x^2}\right)\\
&=(1-(e_0a)^2\frac{\partial^2}{\partial x^2})(I_0\ddot{u}-I_1\frac{\partial \ddot{w}}{\partial x})\\
&\delta w: \quad \frac{\partial^2}{\partial x^2}\left(B_{xx}(x)\frac{\partial u}{\partial x}\right)-\frac{\partial^2}{\partial x^2}\left(D_{xx}(x)\frac{\partial^2 w}{\partial x^2}\right)\\
&+(1-(e_0a)^2\frac{\partial^2}{\partial x^2})\frac{\partial}{\partial x}(N^R(x)\frac{\partial w}{\partial x})\\
&=(1-(e_0a)^2\frac{\partial^2}{\partial x^2})(\frac{\partial}{\partial x}(I_1\ddot{u})-\frac{\partial}{\partial x}\left(I_2\frac{\partial \ddot{w}}{\partial x}\right)+I_0\ddot{w})
\end{aligned} \tag{17}$$

Moreover, the following boundary conditions are obtained as follows:

$$\begin{aligned}
&N_{xx}^{nl}(x)=A_{xx}(x)\frac{\partial u}{\partial x}-B_{xx}(x)\frac{\partial^2 w}{\partial x^2}\\
&+(e_0a)^2\frac{\partial}{\partial x}\left(I_0\ddot{u}-I_1\frac{\partial \ddot{w}}{\partial x}\right)\ \ or\ \ u=0\ at\ x=0,L\\
&M_{xx}^{nl}(x)=B_{xx}(x)\frac{\partial u}{\partial x}-D_{xx}(x)\frac{\partial^2 w}{\partial x^2}\\
&+(e_0a)^2\left(\frac{\partial}{\partial x}(I_1\ddot{u})-\frac{\partial}{\partial x}\left(I_2\frac{\partial \ddot{w}}{\partial x}\right)-\frac{\partial}{\partial x}\left(N^R(x)\frac{\partial w}{\partial x}\right)\right.\\
&\left.+I_0\ddot{w}\right)\ or\ \frac{\partial w}{\partial x}=0\ at\ x=0,L\\
&\frac{\partial M_{xx}^{nl}(x)}{\partial x}+N^R(x)\frac{\partial w}{\partial x}-I_1\ddot{u}+I_2\frac{\partial \ddot{w}}{\partial x}\\
&=0\ \ or\ \ w=0\ at\ x=0,L
\end{aligned} \tag{18}$$

In order to investigate the harmonic vibrations of the present nanobeam, the displacement fields are considered as follows:

$$u(x,t)=u_0(x)e^{i\omega t}, w(x,t)=w_0(x)e^{i\omega t} \tag{19}$$

where ω is the natural frequency, non-dimensional relations are used to obtain the dimensionless equations in the following form:

$$\begin{aligned}
&\delta=\frac{R}{L}\ ,\bar{E}_{mc}=\frac{E_m}{E_c}\ ,\bar{z}=\frac{z}{h_0}\ ,\xi=\frac{x}{L}\ ,\eta=\frac{h_0}{L}\\
&,\bar{u}=\frac{u_0}{L},\bar{w}=\frac{w_0}{L}\ ,\bar{\rho}_{mc}=\frac{\rho_m}{\rho_c},\tau=\frac{\mu}{L},\\
&\Psi^2=\frac{12\rho_c}{E_c}\frac{L^4}{{h_0}^2}\omega^2\ ,\ \phi^2=\frac{12\rho_c}{E_c}\frac{L^4}{{h_0}^2}\Omega^2\\
&\bar{E}(\xi,\bar{z})=\bar{E}_{mc}+(1-\bar{E}_{mc})\times\left(\frac{1}{2}+\bar{z}\right)^{n_z}\times(\xi)^{n_x}\\
&\bar{\rho}(\xi,\bar{z})=\bar{\rho}_{mc}+(1-\bar{\rho}_{mc})\times\left(\frac{1}{2}+\bar{z}\right)^{n_z}\times(\xi)^{n_x}\\
&(\bar{I}_0(\xi),\bar{I}_1(\xi),\bar{I}_2(\xi))=\int_{-\frac{1}{2}}^{\frac{1}{2}}(1,\bar{z},\bar{z}^2)\bar{\rho}d\,\bar{z}\\
&(\bar{A}_{xx}(\xi),\bar{B}_{xx}(\xi),\bar{D}_{xx}(\xi))=\int_{-\frac{1}{2}}^{\frac{1}{2}}(1,\bar{z},\bar{z}^2)\bar{E}d\,\bar{z}\\
&\bar{N}^R=\int_{\xi}^{1}((\delta+\xi)\int_{-\frac{1}{2}}^{\frac{1}{2}}\bar{\rho}d\,\bar{z})d\xi
\end{aligned} \tag{20}$$

By inserting Eqs. 19 and 20 into Eqs. 17 and 18 and applying some mathematical manipulations, the dimensionless forms of the governing equations and related boundary conditions can be rewritten as follows:

$$\begin{aligned}
&\delta u: \ -12\frac{\partial}{\partial\xi}\left(\bar{A}\frac{\partial\bar{u}}{\partial\xi}-\eta\bar{B}\frac{\partial^2\bar{w}}{\partial\xi^2}\right)\\
&=\Psi^2\left(1-\tau^2\frac{\partial^2}{\partial\xi^2}\right)\left\{\eta^2\bar{I}_1\bar{u}-\eta^3\bar{I}_2\frac{\partial\bar{w}}{\partial\xi}\right\}\\
&\delta w: \ -12\frac{\partial^2}{\partial\xi^2}\left(\bar{B}\frac{\partial\bar{u}}{\partial\xi}-\eta\bar{D}\frac{\partial^2\bar{w}}{\partial\xi^2}\right)\\
&-\phi^2\eta\left(1-\tau^2\frac{\partial^2}{\partial\xi^2}\right)\frac{\partial}{\partial\xi}\left(\bar{N}^R\frac{\partial\bar{w}}{\partial\xi}\right)\\
&=\Psi^2\left(1-\tau^2\frac{\partial^2}{\partial\xi^2}\right)\left\{\eta^2\frac{\partial}{\partial\xi}(\bar{I}_2\bar{u})-\eta^3\frac{\partial}{\partial\xi}\left(\bar{I}_1\frac{\partial\bar{w}}{\partial\xi}\right)\right.\\
&\left.+\eta\bar{I}_1\bar{w}\right\}
\end{aligned} \tag{21}$$

Related boundary conditions are:

$$\begin{aligned}
&N_{xx}^{nl}(x)=12\left(\bar{A}\frac{\partial\bar{u}}{\partial\xi}-\eta\bar{B}\frac{\partial^2\bar{w}}{\partial\xi^2}\right)\\
&-\eta^2\tau^2\Psi^2\frac{\partial}{\partial\xi}\left(\bar{I}_1\bar{u}-\eta\bar{I}_2\frac{\partial\bar{w}}{\partial\xi}\right)=0\quad or\quad\bar{u}=0\ at\ \xi=0,1\\
&M_{xx}^{nl}(x)=12\left(\bar{B}\frac{\partial\bar{u}}{\partial\xi}-\eta\bar{D}\frac{\partial^2\bar{w}}{\partial\xi^2}\right)\\
&-\eta\tau^2\Psi^2(\eta\frac{\partial}{\partial\xi}(\bar{I}_2\bar{u})-\eta^2\frac{\partial}{\partial\xi}\left(\bar{I}_3\frac{\partial\bar{w}}{\partial\xi}\right)+\bar{I}_1\bar{w})\\
&-\eta\ \ \tau^2\,\phi^2\frac{\partial}{\partial\xi}\left(\bar{N}^R\frac{\partial\bar{w}}{\partial\xi}\right)=0\quad or\quad\bar{w}=0\ at\ \xi=0,1\\
&12\frac{\partial}{\partial\xi}\left(\bar{B}\frac{\partial\bar{u}}{\partial\xi}-\eta\bar{D}\frac{\partial^2\bar{w}}{\partial\xi^2}\right)\\
&+\phi^2\eta\left(1-\tau^2\frac{\partial^2}{\partial\xi^2}\right)\left(\bar{N}^R\frac{\partial\bar{w}}{\partial\xi}\right)\\
&+\Psi^2\eta\left\{\left(1-\tau^2\frac{\partial^2}{\partial\xi^2}\right)\left(\eta\bar{I}_2\bar{u}-\eta^2\bar{I}_3\frac{\partial\bar{w}}{\partial\xi}\right)-\tau^2\frac{\partial}{\partial\xi}(\bar{I}_1\bar{w})\right.\\
&\left.\right\}=0\quad or\quad\frac{\partial\bar{w}}{\partial\xi}=0\ at\ \xi=0,1
\end{aligned} \tag{22}$$

3. Solution Process

It is difficult to obtain an analytical solution for the free vibration of bi-directional functionally graded nanobeam considering various boundary conditions due to the extreme coupling of the governing equations. Hence, the GDQ method is used to obtain the natural frequency response. Recently, many researchers have used this method due to low computational cost and remarkable convergence in low degrees of freedom[31, 32, 37]. In this method, the derivative of a function f(x) can be written as:

$$\frac{d^m f(X_i)}{dX^m}=\sum_{j=1}^{j=N}C_{ij}^m f_j\qquad(i=1,2,\dots N) \tag{23}$$

where N is several grid points in the x-direction, and the position of each point is determined by the Chebyshev-Gauss-Lobatto technique as:

$$X_i = \frac{1 - cos[(i-1)\pi/(N-1)]}{2} \quad (i = 1,2,\dots N) \tag{24}$$

Also, C_{ij}^{m} are the weighting coefficients along the x-direction, and the first weighting coefficient is calculated as:

$$\begin{aligned} C_{ij}^{(1)} &= \frac{M(X_i)}{(X_i - X_j)M(X_j)} \quad (i,j = 1,2,\dots N \text{ and } i \neq j) \\ C_{ij}^{(1)} &= -\sum_{j=1,i\neq j}^{j=N} C_{ij}^{(1)} \quad (i = j) \end{aligned} \tag{25}$$

where $M(X_i)$ is determined as:

$$M(X_i) = \prod_{j=1,j\neq i}^{N} (X_i - X_j) \tag{26}$$

In addition, the recurrence relationship is used to calculate the higher-order weighting coefficients as follows:

$$C_{ij}^{m} = \sum_{k=1}^{k=N} C_{ik}^{(m-1)} C_{kj}^{(1)} \tag{27}$$

where m is the order derivative of a function; finally, by implementation the GDQ method on boundary condition equations and assembling the governing equations and related boundary conditions equations, the eigenvalues problem are obtained as:

$$\begin{bmatrix} [K_{dd}] & [K_{db}] \\ [K_{bd}] & [K_{bb}] \end{bmatrix} \begin{Bmatrix} \{\lambda_d\} \\ \{\lambda_b\} \end{Bmatrix} = \Psi^2 \begin{bmatrix} [M_{dd}] & [M_{db}] \\ [M_{bd}] & [M_{bb}] \end{bmatrix} \begin{Bmatrix} \{\lambda_d\} \\ \{\lambda_b\} \end{Bmatrix} \tag{28}$$

The values of dimensionless natural frequencies are calculated by solving the eigenvalue problem.

4. Numerical results

This section presents the vibrational behavior of the Euler-Bernoulli nanobeam made of bi-directional functionally graded materials for general boundary conditions with developed Matlab code. The material properties of the bi-directional FG nanobeam are given in Table 1. Convergence studies and validation are carried out to attain sufficient numbers of grid points. Finally, it graphically shows the effects of nonlocal parameters, power-law indexes, nx, nz, and hub ratio.

Table 1. Material properties

Material	*E(Pa)*	$\rho(kg/m^3)$
SUS304	201.04×10^9	8166
Al_2O_3	349.55×10^9	3800

4.1. Convergence and validation

Considering the accuracy dependence of the numerical results on the number of grid points obtained from the GDQ method, convergence studies on the first non-dimensional frequency are performed to determine the required grid numbers for different boundary conditions in Table 2. In the convergence test, various dimensionless parameters such as τ,δ, ϕ and η are considered, represented nonlocal parameter, non-dimensional hub ratio, non-dimensional angular velocity, and thickness to length, respectively. The dimensionless format of mentioned parameters is shown in Eq. 20. It is observed from Table 2 that all numerical results may be converged in N=16. Obtained numerical results are compared with those available in the literature for the first non-dimensional frequency, which demonstrates acceptable accuracy for all different numerical results. Moreover, Fig. 2 shows the results for evaluating the non-dimensional natural frequency and its comparison with Ref [39] under the S-S boundary condition. The non-dimensional parameters are considered as:

$n_z = 1, \eta = 0.1$

Furthermore, good agreement between the obtained results can be seen.

4.2. Parametric study

In this section, the free vibration analysis of rotating bi-directional functionally graded Euler-Bernoulli nanobeam is presented. The effect of various parameters, namely AFG and CFG power indexes and nonlocal and rotary parameters, is studied for C-S, C-C, and C-F boundary conditions. Figs. 3-6 depict the effect of non-dimensional angular velocity on the first non-dimensional frequency versus the AFG index considering different nonlocal parameters under C-C, C-S, and C-F boundary conditions, respectively. In these figures, the invariable values of n_z, δ, and η are selected as 1, 0, and 0.05, respectively. As can be observed, by increasing the angular velocity, the natural frequency of the nanobeam increases. In other words, the stiffness of the 2D-FG nanobeam increases for all the mentioned boundary conditions. Increasing the power-law index decreases the natural frequency due to the variation of the material properties from ceramic to metal and Young's modulus. For n_x >2, increasing n_x has a much slower effect on the fundamental frequency and converges to a constant value. The values of frequency for the C-C beam are higher than those for the remaining boundary conditions. The reason is that the C and F boundary conditions have the fewest and most degree of freedom.

Table 2. Convergence study and verification

				Number of grid points				ref
BC	τ	δ	ϕ	10	14	16		
CF	0.4	1	1	4.81	4.70	4.70	4.70	[36]
CC	0	0	5	24.55	24.55	24.55	24.54	[24]
CS	0	0	5	17.62	17.62	17.62	17.61	[24]

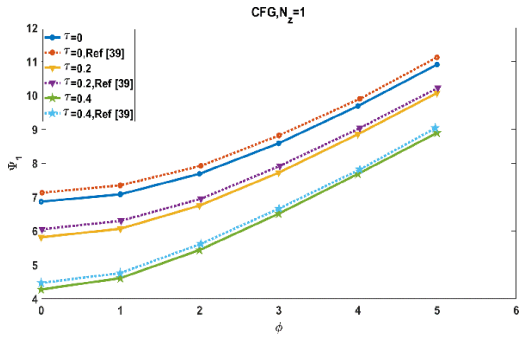

Fig. 2. Comparison of natural frequency parameter results with Ref [39]

Increasing the angular velocity has different trends for the first natural frequency depending on the nonlocal parameter. By observing Figs. 3 and 4, it can be understood that increasing the angular velocity leads to switching the stiffness-softening effect of the nonlocal parameter to the stiffness-hardening effect related to C-C and C-S boundary conditions, respectively. This trend has also been observed for the isotropic nanobeam by Talebitooti et al. [24]. Below a specific value (here $\Phi \approx 6$), the natural frequency decreases by increasing the nonlocal parameter, whereas, for the larger Φ, it increases. Increasing the angular velocity with fundamental frequency is not monotonous and depends upon the boundary condition. Interchanging behavior of nonlocal parameter happens faster for C-C beam.

Figure 5 shows the variation of the first non-dimensional natural frequency under the C-F boundary condition. It is seen that increasing the nonlocal parameter results in the stiffness-hardening effect in contrast with the other boundary conditions. By increasing the angular velocity and the stiffness-hardening effect of the nanobeam, the effect of the nonlocal parameter becomes more noticeable and does not switch. Similar to this result, it was also reported for the isotropic nanobeam by Murmu et al. [35]. It can be concluded from Figs. 3-5 that increasing the angular velocity has a stiffness-hardening effect on the nanocal parameter. In other words, it eliminates the stiffness-softening effect for C-C and C-S boundary conditions and increases the stiffness-hardening effect for the C-F. The comparison of the results in Fig. 5 for different Φ shows that for Φ >6, the effect of axial FG index becomes to be inconsiderable on the fundamental frequency. By making a comparison between Figs. 3 to 5, it can be shown that for the C-F beam, the effect of velocity dominates on the effect of n_x that is much more noticeable than those for other boundary conditions. The main reason that can interpret this phenomenon is that increasing the angular velocity has a more significant effect on increasing the natural frequency of C-F nano-beams than those of other boundary conditions. As $\phi = 9$, the natural frequency increases by approximately four times in comparison to $\phi = 0$. While in other boundary conditions, it increases by approximately two times. As a result, the stiffness-softening effect of the n_x index decreases more rapidly in the C-F boundary condition than those in other boundary conditions.

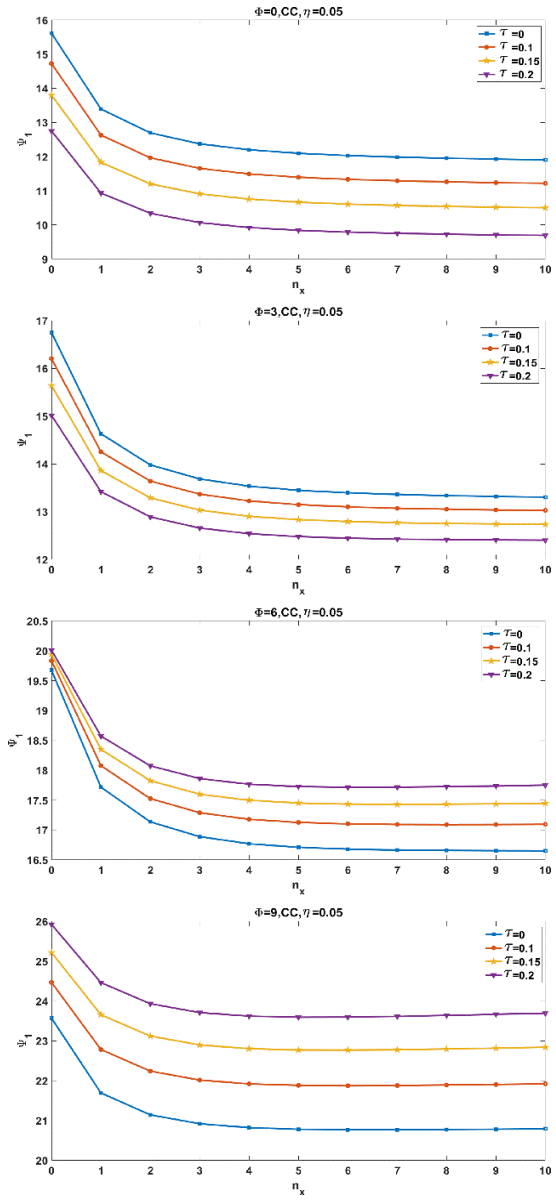

Fig. 3. The effect of non-dimensional angular velocity on the first non-dimensional frequency of C-C nanobeam concerning the AFG index with consideration different nonlocal parameters

Figure 6 shows the effect of the hub ratio on the first non-dimensional natural frequency for the C-C boundary condition. It is mentioned that the CFG index is constant, and the only axial FG index varies. The linear relations are indicated for δ and ψ_1. The investigation of this figure shows that by increasing the hub ratio, the first nondimensional frequency increases that is caused by the rising of the beam's stiffness. By increasing the angular velocity and hub ratio simultaneously, the increasing effect of the hub ratio on the first non-dimensional natural frequency happens more rapidly. Again, the effect of this parameter on the first non-dimensional natural frequency can be observed in Fig. 6.

On the other hand, the CFG index can vary, and the AFG index is kept constant, Fig. 7. In this figure, the hub ratio acts as Fig. 6. By comparing Figs. 6 and 7, it is revealed that the effect of the AFG index is more significant than that of the CFG index in higher angular velocities. In other words, the effect of n_z disappears in higher angular velocities, and the results related to the thickness FG index become closer to each other than those related to the axial FG index.

5. Conclusions

In this study, a nonlocal elasticity theory is developed to study the vibrational behavior of rotary bi-directional functionally graded Euler-Bernoulli nanobeam, including C-C, C-S, and C-F conditions. The prime objective of the current study is the utilization of a bi-directional functionally graded material model in the analysis of rotating nanobeam. The governing equations are solved to obtain the frequency response by using the GDQ method. The effects of material variation, thickness and length direction, nonlocal parameters, angular velocity, and hub ratio are reported. The most important results are shown as follows:

1- As the angular velocity rises, the natural frequency increases.
2- Increasing the FG indexes along x and z directions lead to a reduction in the natural frequencies.
3- The frequency is less affected for n_x >2.
4- The frequency value is in the order of C-C>C-S>C-F which can be attributed to the degree of freedom as F>S>C.
5- Increasing the rotary velocity up to $\Phi \approx 6$ causes the interchanging behavior of nonlocal parameters from stiffness-softening to stiffness-hardening for C-C and C-S beams.
6- In C-F, increasing the angular velocity reinforces the stiffness-hardening effect of the nonlocal parameter.
7- For C-F, the variation of n_x has no significant effect on the fundamental frequency in high angular velocity.
8- By enhancing the angular velocity, the effect of n_z is vanished faster than those of n_x in C-C nanobeam.

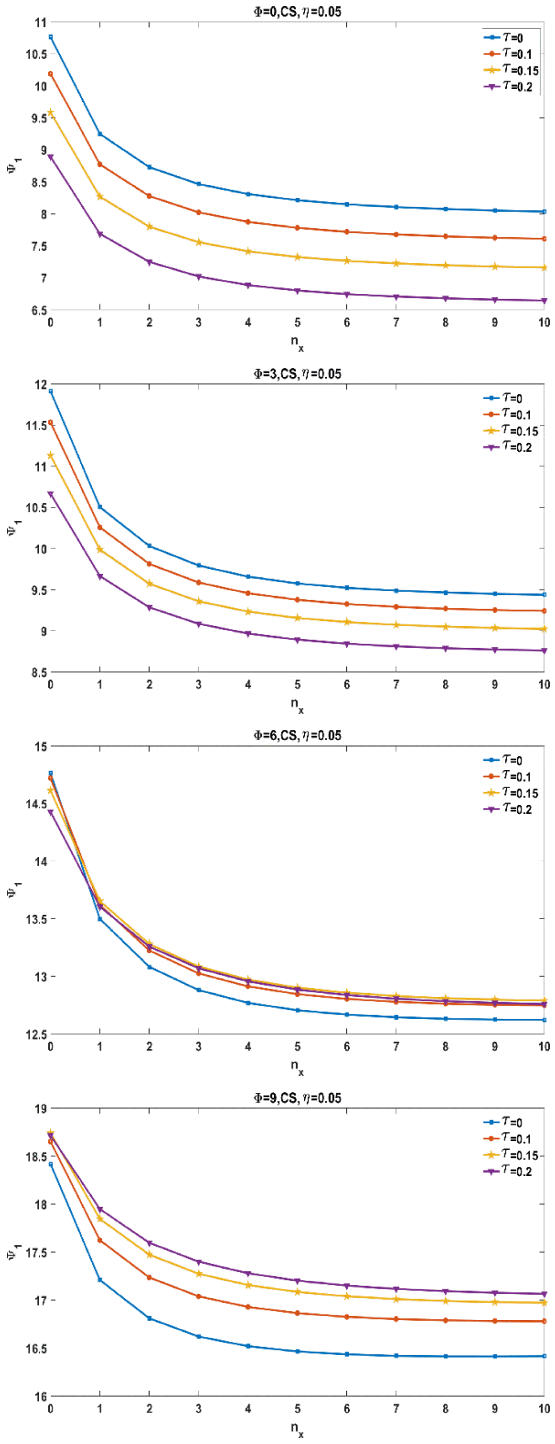

Fig. 4. The effect of non-dimensional angular velocity on the first non-dimensional frequency of C-S nanobeam concerning the AFG index with consideration different nonlocal parameters

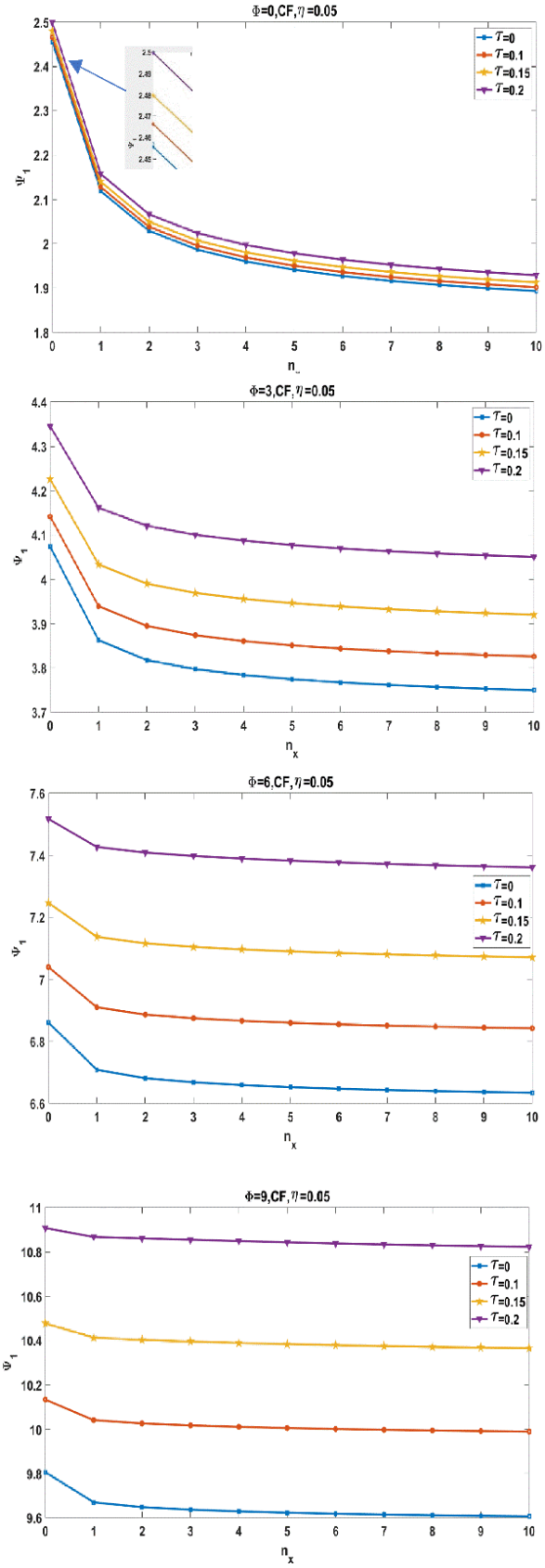

Fig. 5. The effect of non-dimensional angular velocity on the first non-dimensional frequency of C-F nanobeam concerning the hub ratio with consideration different conventional FG index

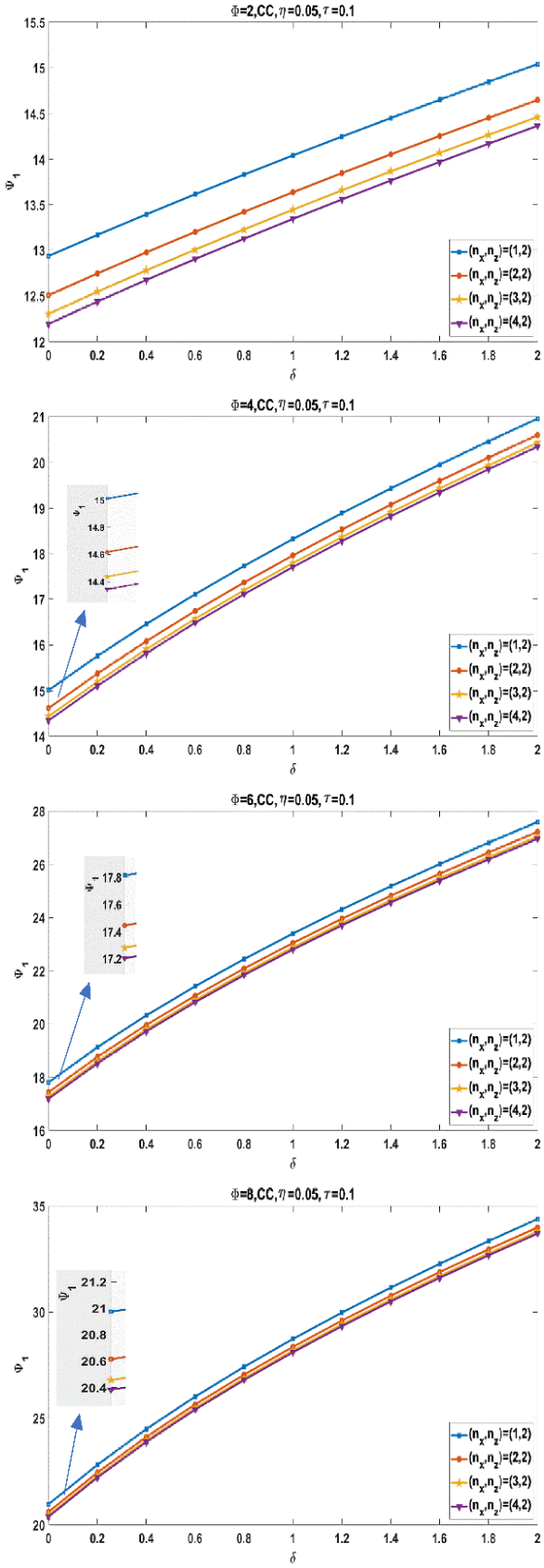

Fig. 6. The effect of non-dimensional angular velocity on the first non-dimensional frequency of C-C nanobeam concerning the hub ratio with consideration different axial FG index

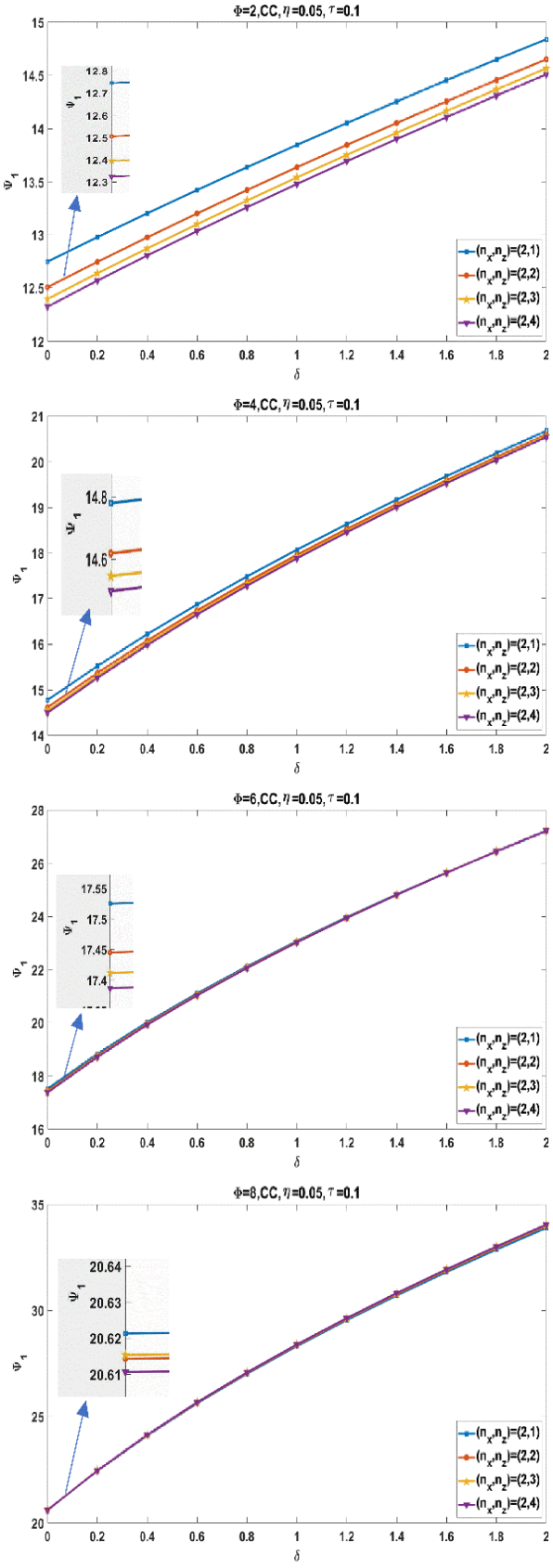

Fig. 7. The effect of non-dimensional angular velocity on the first non-dimensional frequency of C-C nanobeam concerning the hub ratio with consideration different conventional FG index

References

[1] Nguyen DK, Nguyen KV, Gan BS, Alexandrov S, 2018. Nonlinear bending of elastoplastic functionally graded ceramic-metal beams subjected to nonuniformly distributed loads. Applied Mathematics and Computation, 333, pp. 443-59.

[2] Vinyas M, Kattimani SC, 2017. Static studies of a stepped functionally graded magneto-electro-elastic beam subjected to different thermal loads. Composite Structures, 163, pp 216-37.

[3] Mirzabeigy A, 2014. Semi-analytical approach for free vibration analysis of variable cross-section beams resting on elastic foundation and under axial force. International Journal of Engineering, 27(3), pp.385-394.

[4] Jafari A, 2015. Size effect on free transverse vibration of cracked nano-beams using couple stress theory. International Journal of Engineering, 28(2), pp.296-304.

[5] Keshavarzian M, Najafizadeh MM, Khorshidi K, Yousefi P, Alavi M, 2020. High-order Analysis of Linear Vibrations of a ModeratleyThick Sandwich Panel With an Electrorheological Core. Mechanics of Advanced Composite Structures, 7(2), pp.177-188.

[6] Mohammadrezazadeh S, Jafari AA, 2020. Active control of free and forced vibration of rotating laminated composite cylindrical shells embedded with magnetostrictive layers based on classical shell theory. Mechanics of Advanced Composite Structures, 7(2), pp.355-369.

[7] Nejati M, Ghasemi-Ghalebahman A, Soltanimaleki A, Dimitri R, Tornabene F, 2019. Thermal vibration analysis of SMA hybrid composite double curved sandwich panels. Composite Structures, 224, pp.111035.

[8] Babaei H, Kiani Y, Eslami MR, 2019. Thermal buckling and post-buckling analysis of geometrically imperfect FGM clamped tubes on nonlinear elastic foundation. Applied Mathematical Modelling, 71, pp.12-30.

[9] Koizumi M, 1997. FGM activities in Japan. Composites Part B: Engineering, 28(1-2), pp.1-4.

[10] Sherafatnia K, Farrahi G, Faghidian SA, 2014. Analytic approach to free vibration and buckling analysis of functionally graded beams with edge cracks using four engineering beam theories. International Journal of Engineering, 27(6), pp.979-90.

[11] Zafarmand H, Kadkhodayan M, 2015. Three-dimensional elasticity solution for static and dynamic analysis of multi-directional

functionally graded thick sector plates with general boundary conditions. Composites Part B: Engineering, 69, pp.592-602.
[12] Adineh M, Kadkhodayan M, 2017. Three-dimensional thermo-elastic analysis of multi-directional functionally graded rectangular plates on elastic foundation. Acta Mechanica, 228(3), pp.881-99.
[13] Adineh M, Kadkhodayan M, 2017. Three-dimensional thermo-elastic analysis and dynamic response of a multi-directional functionally graded skew plate on elastic foundation. Composites Part B: Engineering, 125, pp.227-40.
[14] Li L, Li X, Hu Y, 2018. Nonlinear bending of a two-dimensionally functionally graded beam. Composite Structures, 184, pp.1049-61.
[15] Li L, Hu Y, 2017. Torsional vibration of bi-directional functionally graded nanotubes based on nonlocal elasticity theory. Composite Structures, 172, pp.242-50.
[16] Zarrinzadeh H, Attarnejad R, Shahba A, 2012. Free vibration of rotating axially functionally graded tapered beams. Proceedings of the Institution of Mechanical Engineers, Part G: Journal of Aerospace Engineering, 226(4), pp.363-79.
[17] Chen Y, Zhang J, Zhang H, 2016. Flapwise bending vibration of rotating tapered beams using variational iteration method. Journal of Vibration and Control, 22(15), pp.3384-95.
[18] Ghadiri M, Shafiei N, Safarpour H, 2017. Influence of surface effects on the vibration behavior of a rotary functionally graded nanobeam based on Eringen's nonlocal elasticity. Microsystem Technologies, 23(4), pp.1045-65.
[19] Ghadiri M, Shafiei N, 2016. Nonlinear bending vibration of a rotating nanobeam based on nonlocal Eringen's theory using differential quadrature method. Microsystem Technologies, 22(12), pp.2853-67.
[20.] Fang J, Gu J, Wang H, 2018. Size-dependent three-dimensional free vibration of rotating functionally graded microbeams based on a modified couple stress theory. International Journal of Mechanical Sciences, 136, pp.188-99.
[21] Fang J, Gu J, Wang H, Zhang X, 2019. Thermal effect on vibrational behaviors of rotating functionally graded microbeams. European Journal of Mechanics-A/Solids, 75, pp.497-515.
[22] Shenas AG, Ziaee S, Malekzadeh P, 2016. Vibrational behavior of rotating pre-twisted functionally graded microbeams in thermal environment. Composite Structures, 157, pp.222-35.
[23] Shenas AG, Ziaee S, Malekzadeh P, 2019. Post-buckling and vibration of post-buckled rotating pre-twisted FG microbeams in thermal environment. Thin-Walled Structures, 138, pp.335-60.
[24] Talebitooti R, Rezazadeh SO, Amiri A, 2019. Comprehensive semi-analytical vibration analysis of rotating tapered AFG nanobeams based on nonlocal elasticity theory considering various boundary conditions via differential transformation method. Composites Part B: Engineering, 160, pp.412-35.
[25] Azimi M, Mirjavadi SS, Shafiei N, Hamouda A, 2017. Thermo-mechanical vibration of rotating axially functionally graded nonlocal Timoshenko beam. Applied Physics A, 123(1), pp.104.
[26] Amiri A, Talebitooti R, Li L, 2018. Wave propagation in viscous-fluid-conveying piezoelectric nanotubes considering surface stress effects and Knudsen number based on nonlocal strain gradient theory. The European Physical Journal Plus, 133(7), pp.1-17.
[27] Amiri A, Vesal R, Talebitooti R, 2019. Flexoelectric and surface effects on size-dependent flow-induced vibration and instability analysis of fluid-conveying nanotubes based on flexoelectricity beam model. International Journal of Mechanical Sciences, 156, pp.474-85.
[28] Li L, Hu Y, 2016. Nonlinear bending and free vibration analyses of nonlocal strain gradient beams made of functionally graded material. International Journal of Engineering Science, 107, pp.77-97.
[29] Ebrahimi F, Shafiei N, 2016. Application of Eringen's nonlocal elasticity theory for vibration analysis of rotating functionally graded nanobeams. Smart structures and systems, 17(5), pp.837-57.
[30] Karamanli A, Aydogdu M, 2019. Size-dependent flapwise vibration analysis of rotating two-directional functionally graded sandwich porous microbeams based on a transverse shear and normal deformation theory. International Journal of Mechanical Sciences, 159, pp.165-81.
[31] Lal R, Dangi C, 2019. Thermomechanical vibration of bi-directional functionally graded non-uniform Timoshenko nanobeam using nonlocal elasticity theory. Composites Part B: Engineering, 172, pp.724-42.
[32] Lei J, He Y, Li Z, Guo S, Liu D, 2019. Postbuckling analysis of bi-directional functionally graded imperfect beams based

on a novel third-order shear deformation theory. Composite Structures, 209, pp.811-29.

[33.] Karami B, Janghorban M, Rabczuk T, 2020. Dynamics of two-dimensional functionally graded tapered Timoshenko nanobeam in thermal environment using nonlocal strain gradient theory. Composites Part B: Engineering, 182, pp.107622.

[34] Golmakani M, Rezatalab J, 2015. Nonuniform biaxial buckling of orthotropic nanoplates embedded in an elastic medium based on nonlocal Mindlin plate theory. Composite Structures, 119, pp.238-50.

[35] Pradhan S, Murmu T, 2010. Application of nonlocal elasticity and DQM in the flapwise bending vibration of a rotating nanocantilever. Physica E: Low-Dimensional Systems and Nanostructures, 42(7), pp.1944-9.

[36] Atanasov MS, Stojanović V, 2020. Nonlocal forced vibrations of rotating cantilever nano-beams. European Journal of Mechanics-A/Solids, 79, pp.103850.

[37] Shafiei N, Mirjavadi SS, MohaselAfshari B, Rabby S, Kazemi M, 2017. Vibration of two-dimensional imperfect functionally graded (2D-FG) porous nano-/micro-beams. Computer Methods in Applied Mechanics and Engineering, 322, pp.615-32.

[38] Eringen AC. Nonlocal polar elastic continua, 1972. International journal of engineering science, 10(1), pp.1-16.

[39] Ehyaei J, Akbarshahi A, Shafiei N, 2017. Influence of porosity and axial preload on vibration behavior of rotating FG nanobeam. Advances in nano research, 5(2), pp.141.